Structural Characteristics of Lightweight Ferrocement Beams with Different Core Material

Abstract:

The main objective of this research is to investigate experimentally the viability and effectiveness of the proposed ferrocement permanent forms and the effect of the test parameters on the behavior of the reinforced concrete ferrocement beams. And investigate the viability of using lightweight materials for the core with the aim of producing light weight structural system. The experimental program comprised casting and testing of eleven reinforced concrete beams of dimensions 200x100x2000mm.These beams are organized in four groups. Group one is the control group in which beams are cast using ordinary formwork and ferrocement. The beams in this group were reinforced with two steel bars of 10 mm at the top and12mm bottom of the beams. The beams in the other three groups were cast using Ferrocement beams. The core of these beams was reinforced with two steel bars of 10 mm diameter at the top and12 mm bottom of the beam. Two types of steel mesh used to reinforce the ferrocement beams namely expanded steel mesh, and welded wires mesh. Single mesh and double layers consisting of mesh together with a strip steel mesh were studied. Three types of core material were investigated: light brick, foam, and light weight concrete admixture with perlite. The test specimens were cast and tested until they failed under flexure load. The performance of the test beams in terms of strength, cracking behavior, ductility, and energy absorption properties was investigated. The use double layer of expanded steel mesh as the additional reinforcement of the main steel can achieved the best performance of the Light weight of ferrocement beams. The results of this research showed that ferrocement beams of light weight cores may be promising as an alternative to conventional beams and may be viable alternatives especially for low-cost residential buildings.

Keywords: ferrocement; composite material; expanded steel mesh, welded wire mesh experimental study.

1. INTRODUCTION

Ferrocement is one of the cementitious composites that are thought to have the ability to address the growing need for complex, high-performing, affordable, and sustainable constructions. Cement-based composites are one of the most popular sustainable construction choices because they need less embodied energy during production and and the number of layers of steel mesh affected the way the U-shaped ferrocement formwork's beams performed [19].

Ferrocement is a top-notch building material for houses. Al-Kubaisy and Jumaat [20] also investigated whether ferrocement cover may be used in the tension zone of reinforced concrete slabs. This material is also used in rehabilitation the reinforcement

application. Its superior strength, crack control, impact resistance, and toughness are demonstrated by several investigations into the physical and mechanical properties of ferrocement, giving it an edge over other thin construction materials [1–8].

This was due to the reinforcement being distributed evenly and closely spaced throughout the material. Because of the short fibers that have been added, ferrocement has improved cracking and stress-strain properties, making it a good building material [9]. Ferrocement presents the opportunity to construct comparatively light prefabricated structural elements that can be reshaped into fascinating architectural forms for affordable homes. Ferrocement has been used to construct silos, roofs, tanks, and to create and restore reinforcing concrete structures. [10–12].

Ferrocement laminates have also been used as permanent forms that eventually become a component of structural elements such as beams and slabs because they are more cost-effective than traditional steel and hardwood formwork [13–16].

The use of ferrocement permanent formwork, particularly for curved structures, was shown to offer excellent potential for expedited construction and material maximizing at low cost. By using steel meshes that increase the structural parts' tensile capacity, it also has the benefit of reducing the amount of tensile reinforcement that is necessary in beams and slabs [17–19]. Investigations were done into how the type of steel mesh elements such as beams, slabs or walls [21,22].

Mourad and Shang test results showed that employing the ferrocement jacket increases the axial load capacity and the axial stiffness of rehabilitation reinforced concrete columns compared to the control columns. they employed ferrocement jacket in repairing rein-forced concrete columns. Numerous studies have been conducted to examine the behavior of ferrocement components (beams, slabs, and columns) under applied loads till failure. For many years, ferrocement has been utilized in place of more expensive materials to restore reinforced concrete and masonry components. It permits quick construction without the use of heavy machinery or highly skilled laborer's, imposes little additional weight, and reduces building costs. These distinctive characteristics enable the use of the data for statistical analysis and comparisons [23] investigated a new mechanical model of polyvinyl alcohol fiber– reinforced ferrocement cementitious composite (PVA-RFCC), which was reinforced with both PVA fiber and steel wire mesh (SWM). A series of experiments were conducted to study their mechanical properties, and a comparative analysis was also performed to evaluate their flexural toughness. The experimental results showed that the flexural properties of the PVA-RFCC specimens can be markedly improved compared with PVA-ECC (PVA-engineered cementitious composites) specimens. The highest increments in the initial stiffness, cracking strength displacement ductility coefficient, and

toughness of the PVARFCC specimens were improved by 62.4%, 174.7%, 251.0%, and 192.5%, respectively. Naser et al. (2020) applied an experimental investigation to study the effect of using different types of reinforcement on the flexural behavior of ferrocement thin hollow core slabs with embedded PVC pipes. Twelve slabs of 1100 × 400 × 55 mm dimensions were casted and tested till failure. The effect of four different types of reinforcement was investigated in this study including; steel wire mesh, macro

Three types of core material were utilized. These types are: light brick core, foam core and light weight concrete admixed with perlite as shown in Table (1), along with the details of the experimental program of all the test specimens. Fig. (1) also reveals all the details of reinforcement for all specimens

3.MATERIALS

·**The fine aggregate:** used in the experimental program was of natural siliceous

and micro steel fibers or a combination of both, steel bars and CFRP bars [24].

According to the findings, of all the tested slabs, the one reinforced just with macro steel fibers had the best flexural strength, while the one reinforced with steel bars had the maximum stiffness and least amount of deflection. Additionally, it was found that the dry design density for all of the hollow core slabs was less than 2000 kg/m3, which is in compliance with the standards for light weight concrete stipulated by the majority of codes of practice.

2.EXPERMENTAL PROGRAM

The experimental program of this research was designed to investigate the feasibility and effectiveness of developing structural ferrocement beam forms filled with different types of core material to be used as a viable alternative to the conventional reinforced concrete beams. The type and number of the reinforcement steel mesh layers in the ferrocement laminate, the type of core material that fills the form and the bonding technique between the form and the core material were varied in the current experimental program to investigate the effect of these test parameters on the strength, stiffness, cracking behavior, ductility, and energy absorption of the tested concrete beams incorporating permanent ferrocement forms. Two types of steel mesh reinforcement were used. These types are: welded wire mesh, and expanded steel mesh. Single and double layers of each type were used.

sand. Its characteristics satisfy the specification ASTM C136-84a. It was clean and nearly free from impurities with a specific gravity 2.65 t/m3 and a modulus of fineness 2.55. [25].

- **The coarse aggregate:** used was crushed dolomite, which satisfied the requirements of the Egyptian Code 203/2007with a specific gravity of 2.75 t/ m^3 and a crushing modulus of 18.5% absorption of 2.1%. The shape of these particles was irregular and angular with a relatively high percentage of elongated particles and a very low percentage of flat particles. [26].

- **The cement:** used was the Ordinary Portland cement, type produced by Al-Amreya cement factory.

- **Silica fume (S.F)**: used to increase the strength of the concrete core and ferrocement mortar. It was employed in mortar formulations as a weight-for-weight partial replacement for cement. The S.F. contained 93% silicon dioxide and had an average particle size of 0.1 micrometers. [28].
- **Fly ash**: used to make cement in proportion. It complies with the applicable international quality criteria for fly ash as well as the chemical and physical requirements of ASTM C618. Fly ash had a Blaine fineness of 330 kg/m2 and a specific gravity of 2.10, which are both relatively low values [29].

- **Water:** To mix and cure the R.C. beams that were subjected to E.C.P. 203/2007

testing, pure, fresh water free of pollutants was utilized.

- **Super plasticizer:** One type of chemical admixtures is used. A high range water reducer (HRWR) (Trade name: Master Glenium RMC 315) is used as plasticizer meeting the requirements of ASTM C494 (type A and

- **Fine expanded perlite**: The term light weight concrete according to ACI is also known as Light density concrete. It is defined as the concrete which is made with light weight coarse aggregate and normal weight fine aggregate with possibly some light weight fine aggregate. This concrete is of density less than 1950

F) [86]. Superplasticizers are used to produce high quality concrete industry. The ability to work with an extremely low w/c ratio allows for the manufacture performance concrete early (18-24 hours) and final strengths. Concrete of high density, low permeability is also produced. Necessary workability needed for the concrete mix. The admixture is a brown liquid. Master Glenium RMC 315 is produced by Passif Company [27].	kg/m3. The aggregate used here has high porosity, small apparent density, more water absorption and low strength. Structural Light Weight Aggregate are typically expanded shale, Clay or slate materials fired in a rotary kiln to develop a porous structure. The technical and chemical properties of Fine Expanded Perlite are shown in table (2).

Table (1) The Details of the Test Specimens.

Group	Specimens Designation	Specimen's Core	Reinforcement details			No. of Layer	Type of Mesh
			Tension Steel bars	Tension Steel bars	Stirrups		
A	A1	———	2 Φ 12	2 Φ 10	Φ6@150mm	———	———
	A2	– ——— –	2 Φ 12	2 Φ 10	Φ6@150mm	- ——— -	———
B	B1	Light Brick	2 Φ 12	2 Φ 10	———	1	Welded Wire Mesh
	B2		2 Φ 12	2 Φ 10	———	2	
	B3	Light Brick Light Brick	2 Φ 12	2 Φ 10	———	2	Welded Wire Mesh Expanded steel Mesh
G	G1	Foam	2 Φ 12	2 Φ 10	———	1	Welded Wire Mesh
	G2	Foam	2 Φ 12	2 Φ 10	———	2	
	G3		2 Φ 12	2 Φ 10	———	2	Welded Wire Mesh Expanded steel Mesh
F	F1	Perlite	2 Φ 12	2 Φ 10	———	1	Welded Wire Mesh
	F2	Perlite	2 Φ 12	2 Φ 10	———	2	
	F3	Perlite	2 Φ 12	2 Φ 10	———	2	Welded Wire Mesh Expanded steel Mesh

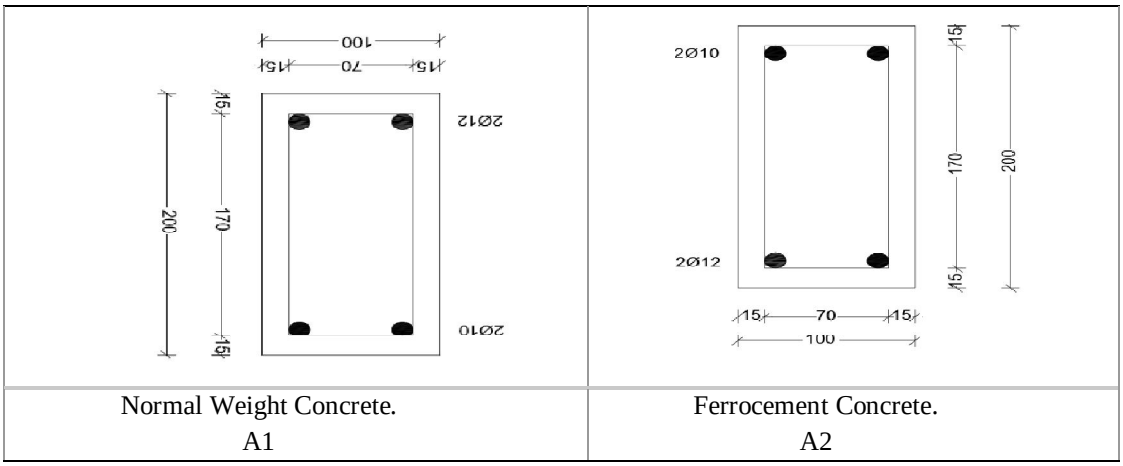

Normal Weight Concrete.	Ferrocement Concrete.
A1	A2

a) Group (A**)**

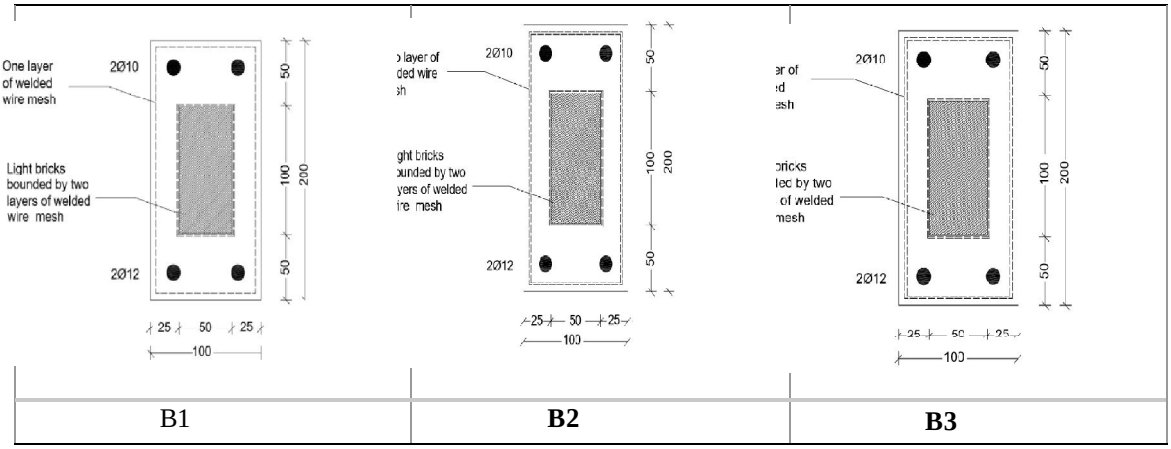

B1	**B2**	**B3**

b) Group (B).

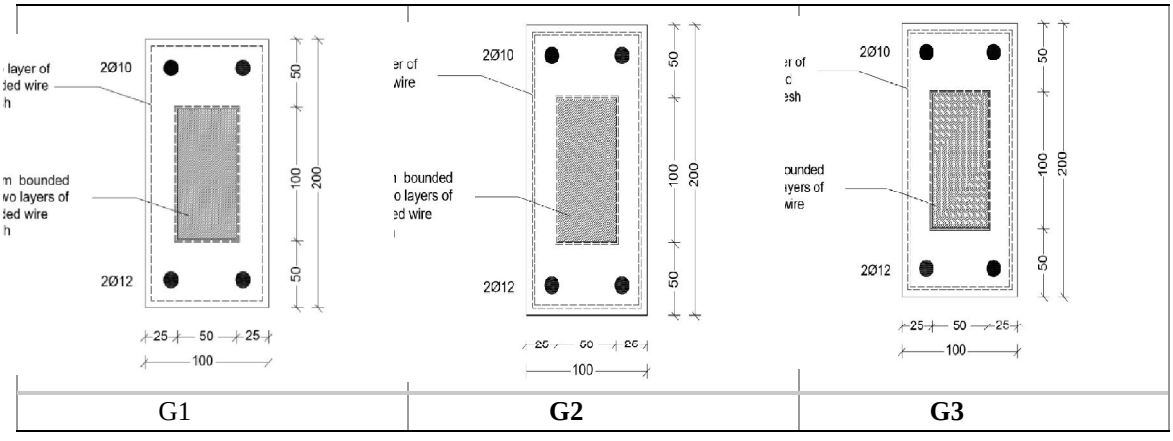

G1	**G2**	**G3**

c) Group (G).

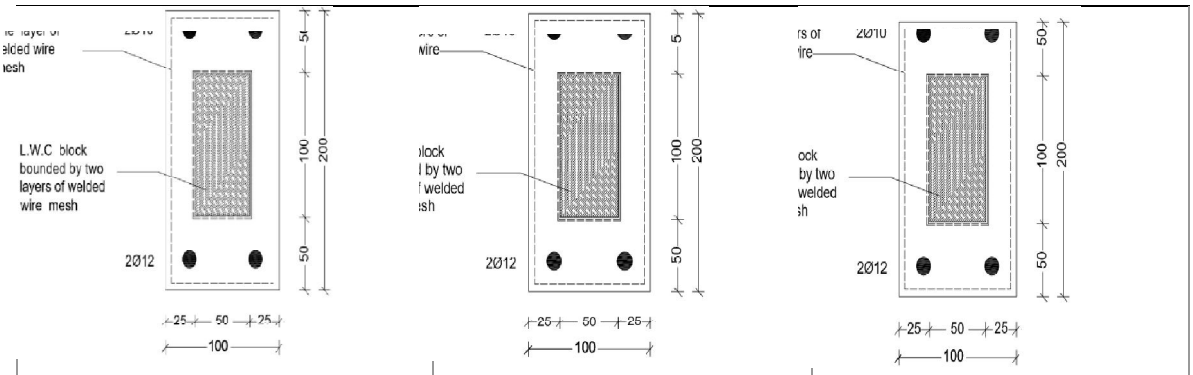

Group (F). (d

Fig. (1): Cross Sections of the Tested Beams

Table (2) Physical Properties of Fine Expanded Perlite [30].

Appearance / Color	Bulk- Density	Moisture
Greyish white	142-149 Kg/m^3	0.1-0.3%

·**Light brick**: Commercially produced light weight brick of dimensions 400x200x70mm. The published technical data of this type of brick shows that it has dry unit weight of 600-650 kg/m^3, porosity of 22-30%, and the average compressive strength was found to be 4.1 MPa. The properties of the used light brick are given in Table (3) **[31].**

·**Foam:** Advefoam is a brand of thermal insulation boards that, in accordance with ASTM C578, are made from high-quality extruded polystyrene foam and come in a variety of thicknesses and edge configurations. The advantages of foam include its high compressive strength, great resistance to chemicals, safety while use, and affordability. The technical of Foam are shown in table (4). Foam produced by CMB Company [32]. Fig. (2) shows the material used to produce the normal weight concrete and ferrocement mortar.

Table (3) Properties of the Light Brick.

Specific Compressive Strength	Average dry Density	Thermal Conductivity	Drying Shrinkage		Porosity	Fire resistance
4 - 5 N/mm^2	600 - 650 kg.m^3	0.27 – 0.34 W/m^{0}c	0.1%		22 – 30%	No deformation occurs till 860^{o}c

Table (4) The Technical Data of Foam [32].

Property	Standard Specification	Unit	Value
Average Density	ASTM D-1622-DIN 53420& ISO 845	K g/m^3	34-36
Thermal Conductivity	ASTM C -518	W / mK	0.028+0.002
(Thermal Conductivity) 5 years aged	DIN 52612	W /m^{0}C	0.0034+0.002
Compressive stress at 10% deflection	ASTM-C165 DIN 5321	K g/cm^2 K Pa	3.0+0.2
Compressive creep (design load) max 2%Deflection after 50 years.	BsEN1606	K Pa	135+5
Water vapor diffusion resistance factor (According to thickness)	DIN 52612	μ	110-225

Silica Fume (a

Fly ash (b

Perlite (c

Light brick (d

Foam (e

Super plasticizer (f

Fig (2): The Material Used to Produce the Normal Weight Concrete and Ferrocement Mortar.

· **Reinforcing steel:** High tensile steel bars with a 12 mm diameter have experienced deformation. Similar to this, high tensile steel bars with a 10 mm diameter were used to reinforce the control beams and the concrete core of the test specimens made up of

·**Expanded steel mesh**: used to bolster cement girders. The technical information and mechanical traits of expanded metal mesh, as supplied by the production business, are listed in Table (3).

ferrocement beams. The ultimate strength of the material was 570 and 730 N/mm2, respectively. Mild steel stirrups with an 8 mm diameter were used to strengthen the control beam against shear. The material's nominal yield stress is 240 N/mm2**.** [33].

· **Welded wire mesh**: this material, which was imported from China, was utilized to reinforce cement girders. The producing company's technical details and welded steel mesh's mechanical characteristics are listed in Table (4). The stress-strain relationship for the expanded steel mesh and the welded wire mesh is shown in Fig (3).

chart(1) Technical Specifications and Mechanical Properties of Expanded Metal Mesh.

tyle	**S heet Size**	**W eight**	**D iamon d Size**	**D imensio n of Strand**	**P roof Stress (N/mm^2)**	**P roof Strain × 10^{-3}**	**Ul timate Strength (N/mm^2)**	**U ltimate Strain× 10^{-3}**
251	1 × 10 m	0 .92 Kg/m^2	1 6 × 31mm	0 .7 × 1.4mm	1 99	9 .7	32 0	5 9.2

chart (2) Technical and Mechanical Properties of Welded Steel Mesh.

Dimensi on size	**Weight (gm/m^2)**	**Proof Stress (N/mm^2)**	**Ultima te Strength (N/mm^2)**	**Ultimate Strain× 10^{-3}**
12.5 × 12.5 mm	430	400	600	1.17

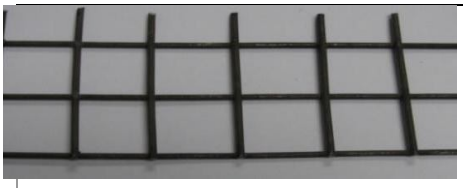

a) Welded wire mesh

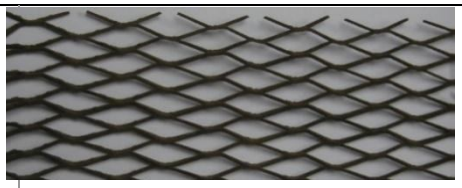

b) Expanded wire mesh

Fig. (3): Types of the Steel Mesh.

3.1 Concrete Mix

The main goal of mix design was to ascertain how a substantial volume of cement might be partially replaced by silica fume and fly ash to boost mortar matrix strength without adversely affecting the mix's quality and attributes in both the fresh and hardened

Cement replacement at 15% by weight, mortar mixtures for the ferrocement was replaced by silica fume and fly ash replaced 20% of the cement's weight in total. After 28 days, the compressive strength was on average 39 MPa. The compressive strength of ferrocement is about 55 MPa. Table (5) provides the mix proportions by weight for regular weight concrete, while Table

phases. In order for the mortar matrix to pass through the layers of steel mesh reinforcement, it was crucial that it had sufficient workability. To improve flow properties and hasten the early strength development, a super plasticizing agent was utilized. Using a water to cement ratio of 0.35, super plasticizer at 1.5% by weight of cement.

provides the mix proportions by weight for ferrocement mortar (6). Perlite was used as a replacement for aggregate in the control concrete at a mass ratio of 30%, giving it a compressive strength of 39 MPa (w/c = 0.35) instead of aggregate. Perlite-containing concrete has a 20 MPa compressive strength. Table (7) lists the mix ratios by weight for the perlite-added light weight concrete.

Table (5) Proportions by Weight of the Normal Concrete Mix.

Material	Cement	Sand	Coarse Aggregates	Water	Silica fume	Superplasticizer	Fly ash
Weight (kg/m^3)	340	680	1360	119	51	5.1	68

Table (6) Proportions by Weight of the Ferrocement Mortar Mix.

Material	Cement	Sand	Water	Silica fume	Superplasticizer	Fly ash
Weight (kg/m^3)	635	1270	222	92.25	9.5	68

The control concrete was designed to have a compressive strength of 39 MPa (w/c = 0.35), and aggregate was replaced by perlite at 30% by mass.

The compressive strength of concrete containing perlite was 20 MPa. The mix proportions by weight of the light weight concrete Admixed with Perlite are given in table (7).

Table (7) Proportions by Weight of the Light Weight Concrete Admixed with Perlite.

Material	Cement	Sand	Coarse Aggregates	Perlite	Water	Silica fume	Superplasticizer
Weight (kg/m^3)	340	680	952	417	119	51	5.1

3.2 Preparation of Test Specimens

The mold from rectangular forms from contras wood with base plate

600x300x9mm. Materials used in concrete mix were prepared and calculated its weight due to design of mix. The ferrocement forms were left for 24 hours in

2200x600x9mm, four side plates 2000x300x9mm, which would be assembled and fixed to the base by screws at the end of each sheet there is a slot 150x10mm high and two transverse end plates of dimensions	**the mold before disassembling the mold. Lastly, the forms were covered with wet burlap for 28 days. All of previous steps are shown in Fig (4).**

a) Wooden mold assembly

b) Reinforcement of group number (A).

b) Reinforcement of group number (B).

c) Reinforcement of group number (G).

d) Reinforcement of group number (F).

e) Mixing Processes of Ferrocement Mortar.

f) Leveling and Curing Concrete Surface.

g) Demoulded Beam.

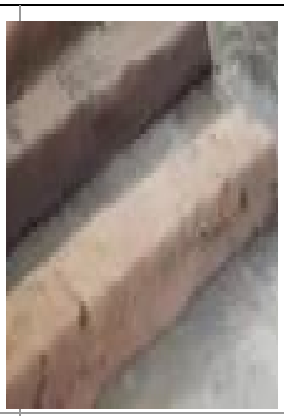

h) Curing Specimens with Wet Burlap.

Fig. (4): Steps of specimen preparation.

3.3 Preparation and Casting of Test Specimens

All beams were put through three lines of testing. The mid-span of the test beam's linear variable displacement transducer (LVDT) was employed to track deflection at the load application location. Situated two centimeters apart from the top and bottom margins, two strain gauges All beams were put through three lines of testing. The mid-span of the test beam's linear variable displacement transducer (LVDT) was employed to track deflection at the load application location. Situated two centimeters apart from the top and bottom margins, two strain gauges.

A small load was then first applied to make sure that all instruments were working. The load was thereafter increased gradually till the failure of the specimen. At each load stage, strains in concrete and the deflections were recorded automatically using a computerized data.

The crack pattern was also noted at each load stages. The ultimate load was identified when excessive cracking occurred at the bottom of the beam, applied load dropped and deflection increased shown in Fig. (4).

a) Hydraulic jack.

b) Strain Gauges set up.

LVDT (**c**

Recording Values Computerized. (d

pic (1): Test specimen set up.

4. Experimental Results

Comparisons are conducted between the results of the different test groups so as to examine. The results of all test specimens are listed in Table (7) shows the obtained experimental results for each specimen as well as the average results for each group. The table shows the obtained results for the first crack load, service load, ultimate load, deflection at ultimate load, ductility ratio, and energy absorption. Ultimate load and deflection at ultimate load were measured and obtained during the test, while the first crack load, service load, ductility ratio and energy absorption were determined from the load-deflection diagram for each specimen.

chart (3) Test Results for all Experimental Beams Tested.

Specimen's Design-action	**Specimen's No.**	**Frist Crack Load (k.N)**	**Service-ability Load (k.N)**	**Ultimate Load (k.N)**	**Frist Crack Deflection (mm)**	**Max Deflection (mm)**	**Ductility Ratio**	**Energy Absorption**
A	A1	7.08	39.627	43.62	1.44	8.467	5.88	287.8
	A2	10.66	46.47	48.17	1.28	8.18	6.39	216.1
B	B1	9.66	38.628	40.63	1.48	7.82	5.28	184.48
	B2	10.32	40.463	47.95	1.55	9.6	6.67	279.05
	B3	13.99	53.83	57.61	1.34	10.00	7.47	319.85
G	G1	11.62	35.53	38.24	1.72	8.69	5.04	248.04
	G2	12.85	35.19	44.07	1.96	10.19	5.21	257.67
	G3	13.50	42.5	52.47	1.93	10.33	5.34	293.37
F	F1	14.21	38.92	51.99	2.63	11.57	5.56	369.41
	F2	15.57	47.31	55.27	1.73	12.32	7.12	439.69

	F 3	1 6.00	44 .53	61 .98	1.6 7	1 2.567	7. 53	45 8.26

4.1 Flexural Serviceability Load

The flexural serviceability load is computed using the load-deflection curves. The load associated with deflection is defined by the Egyptian Code as the girder's span (1800 mm) divided by (constant=250). The values for the ultimate load, serviceability load, and first cracking load for each tested beam are shown in Fig. (5). The major goal of serviceability load estimation is to examine how different meshes affect the outcomes.

4.2 Ductility Ratio

The mid span deflection at the ultimate load to that at the first crack load is used to compute the ductility ratio. At B2, B3, and F2 and F3, reinforced beams with welded steel meshes and expanded metal meshes have better ductility ratios than control beams. In comparison to control beams, beams B1, G1, G2, G3, and F1 have a lower ductility ratio. However, of all the examined beams, beam F3 had the highest ductility index. Fig. (6) shows ductility ratios for all beam tested**.**

4.3 Energy Absorption

The area beneath the load- deflection curve is referred to as energy absorption. The area under the load-deflection curve using a Microsoft office (excel sheet) by integrating the equation of the load – deflection curve specimen as follows: ultimate load Energy absorbed = $\int^{\Delta u} f(\Delta)\, d\Delta$; where f(Δ) is equation of load – deflection Δu is mid span deflection at failure load. The energy absorption of beams reinforced with expanded steel mesh was greater than that of control beam. Fig. (7) emphasizes energy absorption for all beams.

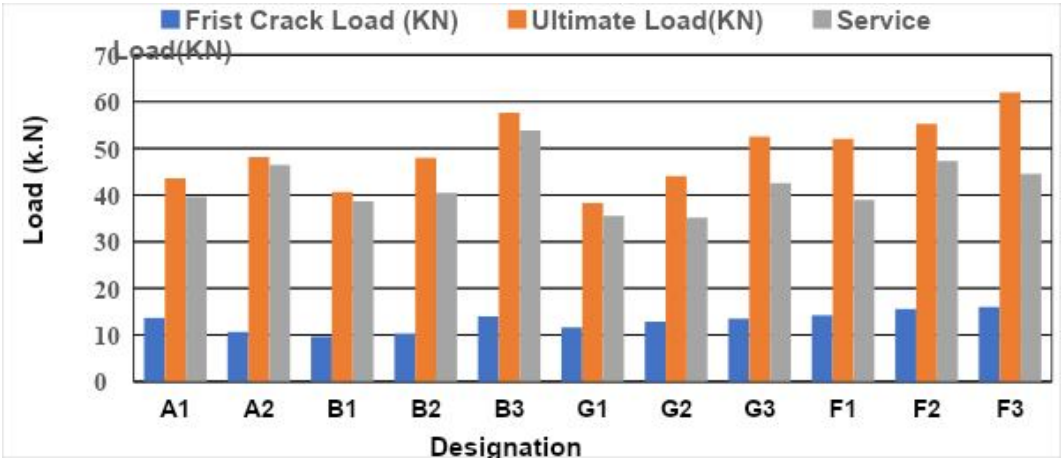

Fig. (5): First Crack, Serviceability and Ultimate loads for All tested Beams.

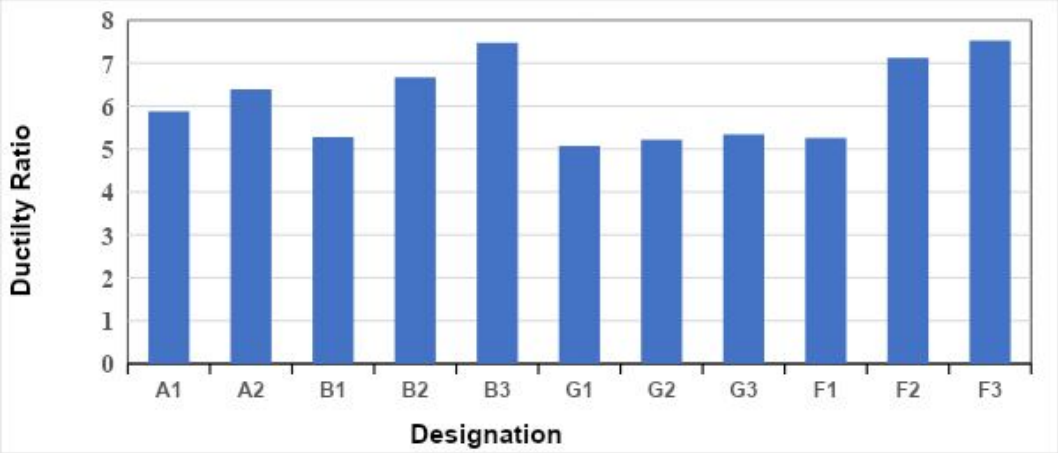

Fig. (6): Ductility Ratio of all Beams Tested.

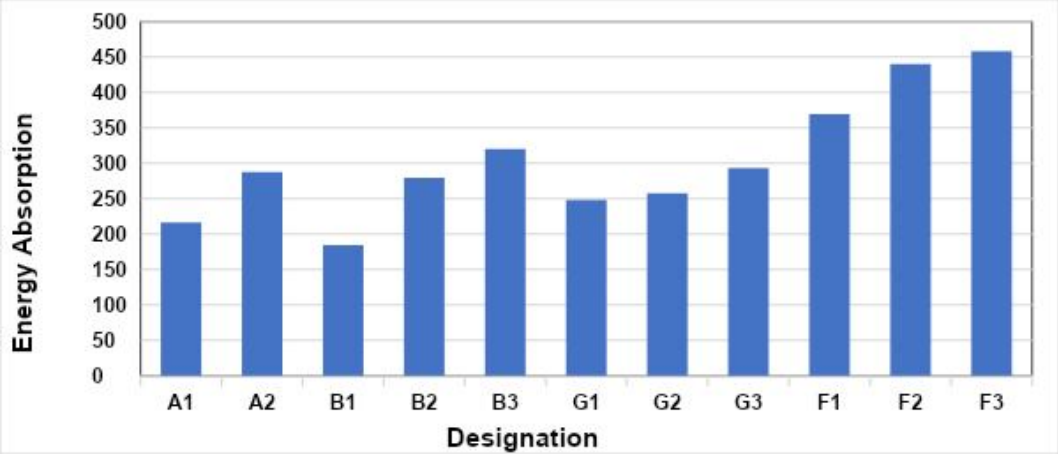

Fig. (7): Energy Absorption for all Beams Tested

4.4 Load-Deflection Relationship

The behavior of the test specimen in terms of load-deflection relationship, compressive and tensile strain and cracking behavior is discussed in the following sections Fig. (8) shows the load -deflection curves of control specimen for normal weight concrete beam (A1) and ferrocement beam (A2). Group A, from figure the ultimate load for specimen (A1) is less than that of the specimen (A2). The percentage of decreasing in the ultimate load is 10.41%. Also, deflection of spacemen (A1) increases by 3.38 % compared to specimen (A2).

From Fig. (9) group (B), group of beams with one type of core material (Foam), and reinforced by two types of mesh reinforcement (expanded steel mesh and welded wire mesh) in additional to steel bars (G1), (G2) and (G3). The ultimate load for specimen (G3) is more than that of specimen (G1, G2). This is due to types of cores, the percentage of increasing in ultimate load is 27.12%, 16 %respectively. Also, the deflection of specimen (G3) is increase by 15.87%,1.27% respectively compared to specimen (G3).

From Fig. (10) group (G), group of beams with one type of core material (Foam), and reinforced by two types of mesh reinforcement (expanded steel mesh and welded wire mesh) in additional to steel bars (G1), (G2) and (G3). The ultimate load for specimen (G3) is more than that of specimen (G1, G2). This is due to types of cores, the percentage of increasing in ultimate load is 27.12%, 16 %respectively. Also, the deflection of specimen (G3) is increase by 15.87%,1.27% respectively compared to specimen (G3).

From Fig. (11) group (F), group of beams with one type of core material (light weight concrete admixed with perlite), and

beams with one type of core material (Light weight brick), and reinforced by two types of mesh reinforcement (expanded steel mesh and welded wire mesh) in additional to steel bars (B1), (B2) and (B3). The ultimate load for specimen (B3) is more than that of specimen (B1, B2). This is due to types of core, the percentage of increasing in ultimate load is 29.74%, and 16.76% respectively. Also, the deflection of specimen (B3) is increase by 21.92%, and 4.09% respectively compared to specimen (B3).	reinforced by two types of mesh reinforcement (expanded steel mesh and welded wire mesh) in additional to steel bars (F1), (F2) and (F3). The ultimate load for specimen (F3) is more than that of specimen (F1, F2). This is due to types of core. the percentage of increasing in ultimate load is 16.1 %, 11.83 % respectively. Also, the deflection of specimen (F3) is increase by 7.96 %,1.97% respectively compared to specimen (F3).

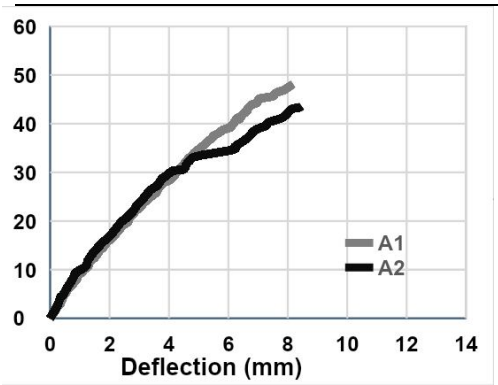

Fig. (8): Load-Deflection Curves for Group (A).

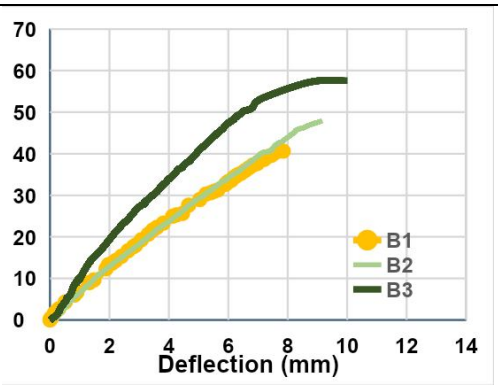

Fig. (9): Load-Deflection Curves for Group (B).

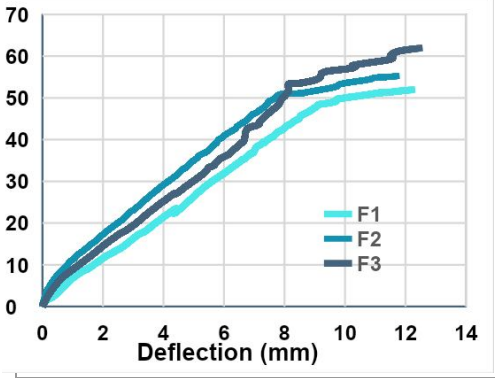

Fig. (10): Load-deflection Curves for Group (F).

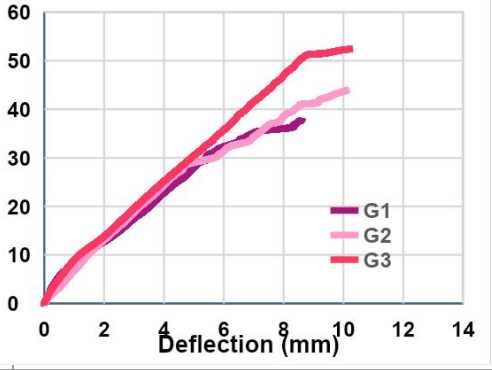

Fig. (11): Load-deflection Curves for Group (G).

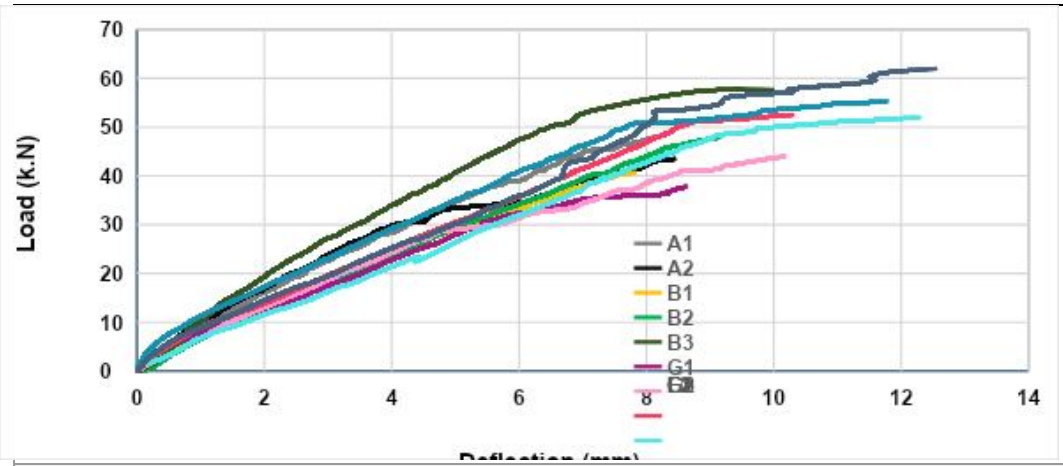

Fig. (12): Load-deflection Curves for all Beams tested.

4.6 The Effect of Using Various Types of Meshes

In order to evaluate of the reinforced steel mesh type at beams with the same core, specimens reinforced with expanded steel mesh and welded wire mesh were compared to control specimens. Fig. (13) illustrate the load deflection curves of control specimens (A1and A2) is compared to the specimen reinforced with two layers of welded wire mesh (B2) the specimen reinforced with two layers of expanded steel mesh (B3). From figure the ultimate load for specimen (B3) is more than that of specimen (A1, A2, and B2). This is due to type of mesh. the percentage of increasing in ultimate load is 24.28%,16.9%, and 20.14 respectively. Also, the deflection of specimen (B3) is increase by 15.62%,18.28%, and %,4.26% respectively.

Fig. (14) illustrate the load deflection curves of control specimens (A1and A2) is compared to the specimen reinforced with two layers of welded wire mesh (G2) the specimen reinforced with two layers of expanded steel mesh (G3). From figure the ultimate load for specimen (G3) is more than

that of specimen (A1, A2, and G2). This is due to type of mesh. the percentage of increasing in ultimate load is 16.96%, 8.20%, and 16% respectively. Also, the deflection of specimen (G3) is increase by18%,20.78%, and 1.27% respectively.

From Fig. (15) illustrate the load deflection curves of control specimens (A1and A2) is compared to the specimen reinforced with two layers of welded wire mesh (F2) the specimen reinforced with two layers of expanded steel mesh (F3). From figure the ultimate load for specimen (F3) is more than that of specimen (A1, A2, and F2). This is due to type of mesh. the percentage of increasing in ultimate load is29.62% ,22.29 %, and 11.83 % respectively. Also, the deflection of specimen (F3) is increase by 32.63%,34.91%, and 1.97% respectively.

Fig. (16) illustrate the load deflection curves of control specimens (A1and A2) is compared to the specimen reinforced with two layers of welded wire mesh (B2), (G2) and (F2). From figure the ultimate load for specimen (F2) is more than that of specimen (A1, A2, B2, and G2). The percentage of increasing in ultimate load is 21.07%,12.86%,13.83%, and 20.27 % respectively. Also, the deflection of specimen (B3) is increase by 31.44%,33.6%,22.07% and %,17.24% respectively.

Fig. (17) illustrate the load deflection curves of control specimens (A1and A2) is compared to the specimen reinforced with two layers of expended steel mesh (B3), (G3) and (F3). From figure the ultimate load for specimen (F3) is more than that of specimen (A1, A2, B3, and G3). The percentage of increasing in ultimate load is 29.62%,22.29%,7.05%, and 15.36 % respectively. Also, the deflection of specimen (B3) is increase by 32.40%,35.37%, 20.35, and %,17.83% respectively.

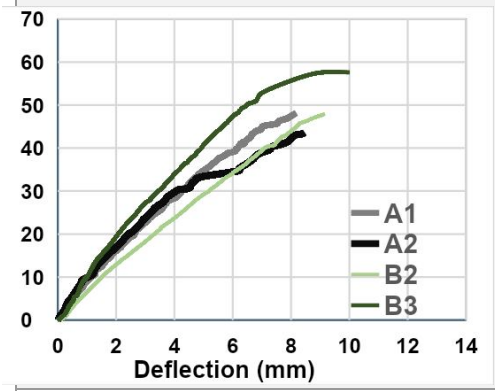

Fig. (13): The Effect of Type of Reinforcement on the Load-Deflection for Group (B).

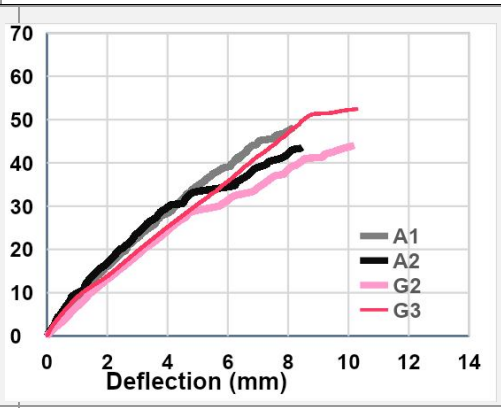

Fig. (14): The Effect of Type of Reinforcement on the Load-Deflection for Group (G).

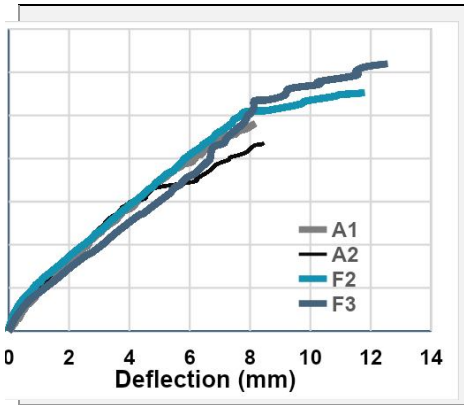

Fig. (15): The Effect of Type of Reinforcement on the Load-Deflection for Group (F).

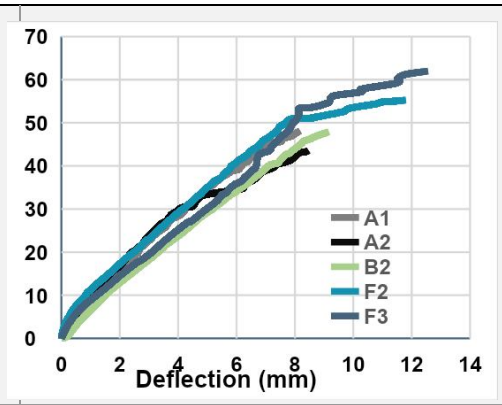

Fig. (16): The Effect of Type of Reinforcement on the Load-Deflection for Welded Wire Mesh.

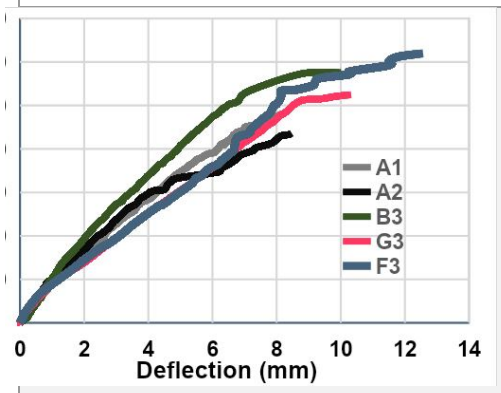

Fig. (17): The Effect of Type of Reinforcement on the Load-Deflection for Expanded steel Mesh.

4.7 The Effect of Load to Weight Ratio

The specific strength is a material's strength (force per unit area at failure) divided by its density. It is also known as the strength-to-weight or load weight ratio. It better from dynamic constructions. Beams F3 gives the maximum load to weight ratio (when load 61.99 t and weight 97kg) for all beam tested. Beam A1 given lower load to weight ratio (when load 43.62 t and weight 104.5kg) than all beams tested. Fig. (18) shows load-weight ratio for all beams.

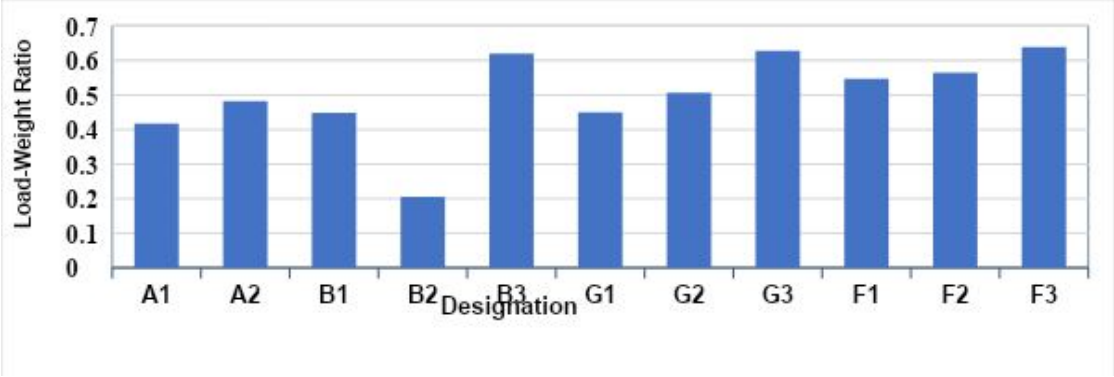

Fig. (18): The Load-Weight Ratio for all tested beam

4.8 Compressive and Tensile Strain

Load stain-compressive and tensile strain curves for Control group (A) specimens (A1and A2) are shown in Fig. (19). The compressive strain in beams increased as the applied load increased. At a maximum load of 43.62 k.N, the maximum compressive strain was at -0.0024. At the same load, the maximum tensile strain was 0.0190. At a maximum load of 48.165K.N, the maximum compressive strain at beam (A2) was around -0.00227. At the same load, the maximum tensile strain was 0.020.

Load stain-compressive and tensile strain curves for group (B) specimens (B1, B2and B3) are shown in Fig. (20). The compressive strain in beams increased as the applied load increased, as seen by the curves. At a maximum load of 40.63 k. N, the maximum compressive strain at beam (B1) was at -0.00181. At the same load, the maximum tensile strain was 0. 01235.The compressive strain in beams increased as the applied load increased, as seen by the curves. At a maximum load of 47.95 k. N, the maximum compressive strain at beam (B2) was at -0.001954. At the same load, the maximum tensile strain was 0.0098. The compressive strain in beams increased as the applied load increased, as seen by the curves. At a maximum load of 57.61 k. N, the maximum compressive strain at beam (B3) was at -0.002377. At the same load, the maximum tensile strain was 0.00827.

Load stain-compressive and tensile strain curves for group (G) specimens (G1, G2and G3) are shown in Fig. (21). The compressive strain in beams increased as the applied load increased, as seen by the curves. At a maximum load of 38.24 k. N, the maximum compressive strain at beam (G1) was at -0.00148. At the same load, the maximum tensile strain was 0.007684. The compressive strain in beams increased as the applied load increased, as seen by the curves. At a maximum load of 44.07 k.N, the maximum compressive strain at beam (G2) was at -0.00122. At the same load, the maximum tensile strain was 0.00768. At a maximum load of 44.07 k. N, the maximum compressive strain at beam (G2) was at -0.00122. At the same load, the maximum tensile strain was 0. 00768.The compressive strain in beams increased as the applied load increased, as seen by the curves. At a maximum load of 52.94 k.N, the maximum compressive strain at beam (G3) was at-0.00218. At the same load, the maximum tensile strain was 0.008844.

Load stain-compressive and tensile strain curves for group (F) specimens (F1, F2and F3) are shown in Fig. (22). The compressive strain in beams increased as the applied load increased, as seen by the curves. At a maximum load of 51.99 k. N, the maximum compressive strain at beam (F1) was at -0.00226. At the same load, the maximum tensile strain was 0. 00119.The compressive strain in beams increased as the applied load increased, as seen by the curves. At a maximum load of 55.05 k. N, the maximum compressive strain at beam (F2) was at -0.00227. At the same load, the maximum tensile strain was 0.00636. The compressive strain in beams increased as the applied load increased, as seen by the curves at a maximum load of 61.98 k. N, the maximum compressive strain at beam (F2) was at -0.0025. At the same load, the maximum tensile strain was 0.0184.

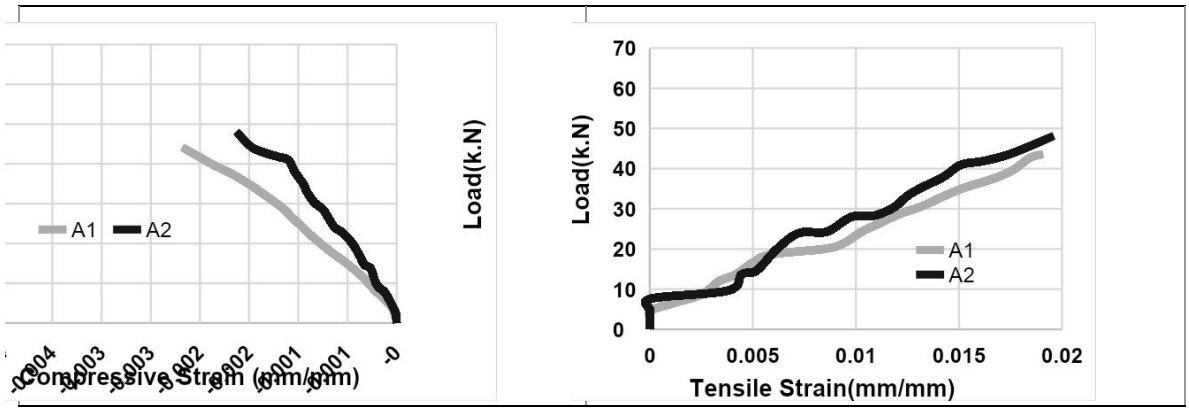

Fig. (19): Load- Compressive and Tensile Strain Curves for group (A).

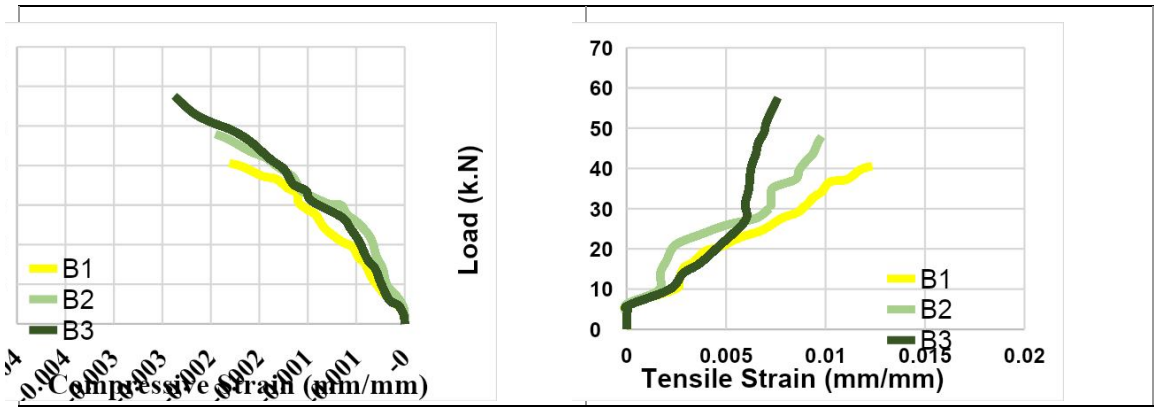

Fig. (20): Load- Compressive and Tensile Strain Curves for group (B).

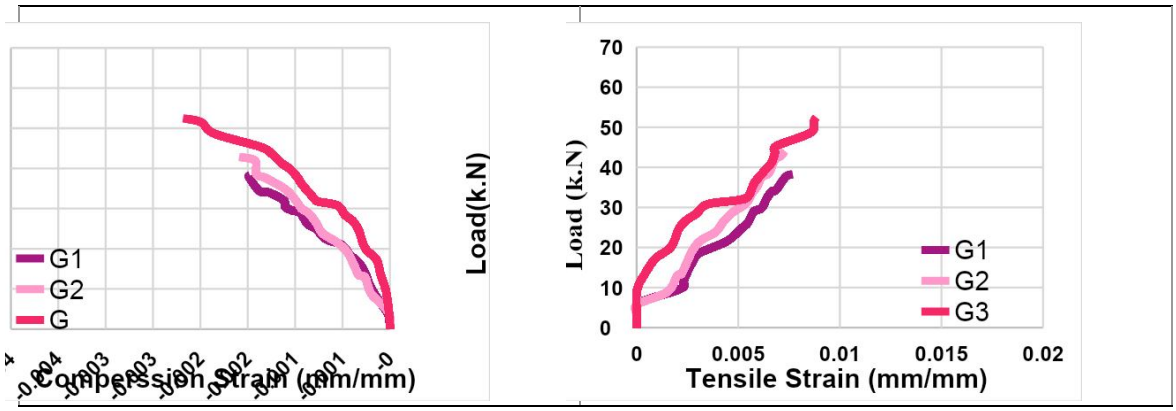

Fig. (21): Load- Compressive and Tensile Strain Curves for group (G).

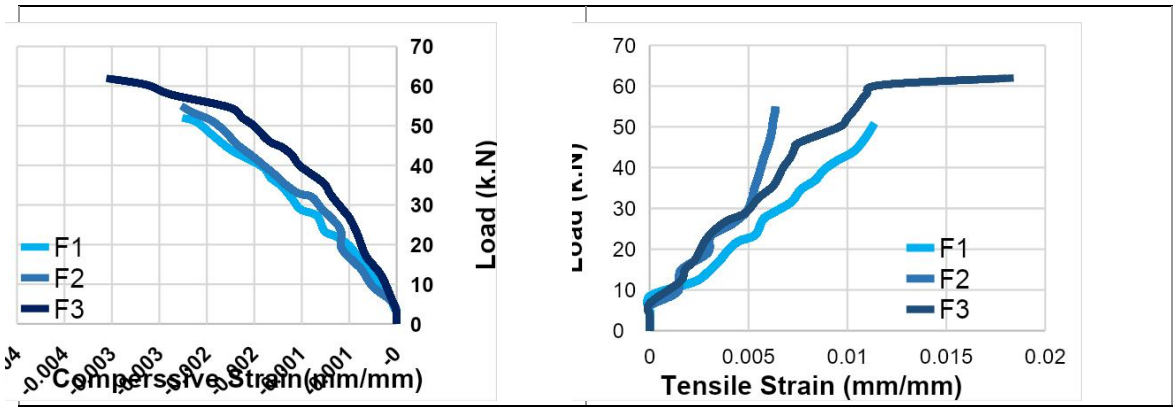

Fig. (22): Load- Compressive and Tensile Strain Curves for group (F).

5. Cracking Patterns and Mode of Failure

Cracks are traced and marked throughout the side of the specimen. The initial crack load of each specimen, crack propagation, and failure mode are recorded. Fig. (23) and shows the crack pattern of control specimens A1 and A2. For control beams A1 and A2, hair cracks were observed to develop first at the bottom edge of the beam's mid span. However, the number of hair cracks in the control beams was limited and the cracks were wider in width and more spaced compared of ferrocement beams, Beam A2 developed finer cracks with smaller width compared with that of Beam A1. While Specimen A1 spalled both at the top and the bottom. Specimen A2 underwent crushing at the top.

Fig. (24) shows the crack pattern of specimens B1, B2, and B3 beams. It was found that flexural cracks developed from around the mid span at the bottom and top of the beams. The cracks were less than those of the control specimens and this could be due to the higher reinforcement which controlled crack width in the ferrocement beams. It was observed that cracks were developed in specimens reinforced with expanded steel mesh, more rapidly than those reinforced with welded wire mesh.

It was observed also that ferrocement beams reinforced with welded wire mesh and core with light weight bricks developed fewer cracks with greater widths than those in the control beams. Failure of the beams in this group occurred only by cracking at the bottom, crushing at the top and no spalling was observed.

Fig. (25) shows the crack pattern of specimens G1, G2, and G3 beams, it was observed that flexural cracks developed from around the mid span of the ferrocement beams and the beams exhibited more crack control compared to the control beams. Beams reinforced with welded wire mesh showed less warnings prior to failure compared to those reinforced by expanded steel mesh, which had more hair cracks but with less crack width.

Fig. (26) shows the crack pattern of specimens F1, F2, and F3 beams reinforced with expanded steel mesh and welded wire mesh. Beams reinforced with expanded steel mesh had a greater number of cracks but with less crack widths than the other specimens in the group. As observed with the previous groups, beams reinforced with welded wire mesh resulted in a brittle failure, fewer cracks with wider crack widths compared with those reinforced with expanded steel mesh.

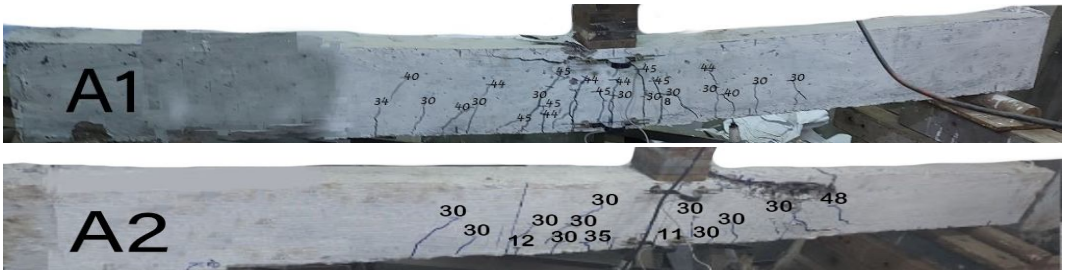

Fig (23): Cracking Patterns for Group (A).

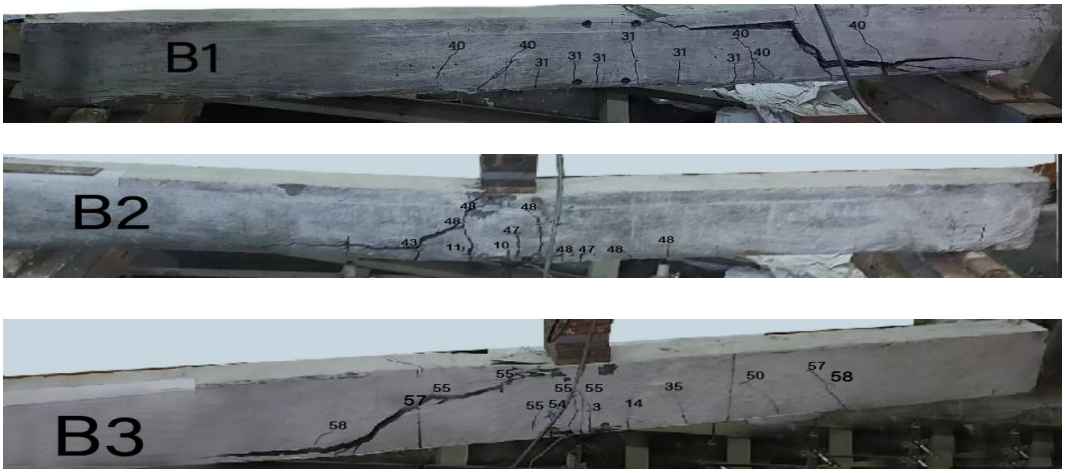

Fig (24): Cracking Patterns for Group (B).

Fig (25): Cracking Patterns for Group (G).

Fig (26): Cracking Patterns for Group (F).

6. Conclusion

The flexural behavior of lightweight ferrocement composite beams under concentrated loads as compared to that of conventional structural reinforced concrete beams were the focus of this research's experimental program. The following conclusions can be drawn:

1. The beams incorporating ferrocement beams and concrete achieved higher first crack load, serviceability load, ultimate load, and energy absorption compared to the control specimen irrespective of the type of steel mesh and number of steel mesh layers.

2. The best behavior of ferrocement beams was that of reinforced with two layers of expanded metal mesh in terms of ultimate load and energy absorption with various type of core.

3. The specimen reinforced with two layers of expanded steel mesh increase the ultimate load by percentage (11.83% ,16% and 20.14%) compared to that reinforced with two layers of welded wire mesh with various type of core.

4. The ferrocement beam with light weight concrete core reinforced with two layers of expanded steel mesh increase the ultimate load by percentage (29.62%, and 22.29%) compared to control beams.

5. Using two layers of expanded metal mesh in reinforced ferrocement beams clearly increase the ultimate moment, decrease deflection, and improve the energy absorption compared to using other types of meshes.

6. The beams with light weight concrete admixed with perlite core achieved higher first crack load, and ultimate load relative to the conventional concrete beams when welded wire mesh was employed. On the other hand, no change in the first crack load and reduction in the ultimate load were achieved when expanded wire mesh was used. Using light weight concrete core resulted in a decrease in the serviceability load and energy absorption relative to the conventional concrete beams reg0ardless of the type of steel mesh used.

7. The ductility ratio increased as a result of using ferrocement beams. The

percentage of increase depends on the type and number of steel mesh layers in the ferrocement beams with various type of core.

.8 The highest ductility ratio property was shared between specimens made of ferrocement beam reinforced with two layers of expanded steel mesh and with the light weight concrete core by percentage (21.8% and 14.8%) compared to control beams.

.9 The ductility ratio for the beams with welded wire mesh reinforcement was less than that with expanded steel mesh.

.10 The highest energy absorption property was shared between specimens made of ferrocement beam reinforced with two layers of expanded steel mesh and with the light weight concrete core by percentage (59.22%) compared to control beams, and the lowest was found mostly with ferrocement beam reinforced with one layer of welded wire mesh and with foam core by percentage (1.94%).

.11 The highest load and weight ratio property was shared between specimens made of ferrocement beam reinforced with two layers of expanded steel mesh and with the light weight concrete core compared to control beams.

.12 The results obtained from the finite element analysis agreed well with the experimental ones for all tested specimens and the high percentage of difference in specimen F1 when the ultimate load in experimental study 51.99 k. N, ultimate load in finite element method 53.488k.N and percentage of difference 2.8 %.

.13 The developed beams utilizing thin ferrocement beam could be successfully used as an alternative to the traditional reinforced concrete beams, which can be of true merit in both developed and developing countries besides its anticipated economic and environmental merits. Further research needs to be conducted to reach sound recommendations for practical use especially for the beams with light brick core and light weight concrete admixed with perlite.

.14 tudy the viability of employing other types of mesh reinforcement in the ferrocement beams such as polypropylene mesh, tensar mesh.

.15 To investigate other means of enhancing the interaction between the ferrocement beams and the light brick core or light weight concrete to prevent possible separation between the two components for example making shear connector to consolidate between concrete and cores.

REFERENCES

.1 A.E. Naaman, Ferrocement and Laminated Cementitious Composites, Techno presses 3000, Ann Arbor, Michigan, 2000.

.2 R. Wrigley, Permanent Formwork in Construction, Construction Industry Research & Information Association (CIRIA), London, 2001.

.3 E. Fahmy, Y. Shahen, M. Abou Zaid, Development of ferrocement panels for floor and wall construction, 5th Structural Specialty Conference of the Canadian Society for Civil Engineering, Canada, 2004.

.4 E.H. Fahmy, Y.B. Shaheen, Z.M.D. Abou, A.M. construction with locally available materials,

Gaafar, Ferrocement sandwich and hollow core panels for wall construction, J. Ferrocement 36 (3) (2006) 876–891.

E.H. Fahmy, Y.B. Shaheen, Z.M.D. Abou, A.M. Gaafar, Ferrocement sandwich and hollow core panels for floor construction, Can. J. Civ. Eng. 27 (1) (2012) 1297–1310. .5

Y. El-Sakhawy, Structural Behavior of Ferrocement Roof Elements [M.Sc. thesis], Menoufia University, Shebin El-Kom, Egypt, 2007. .6

N.R. Husein, V.C. Agarwal, A. Rawat, An experimental study on using lightweight web sandwich panel as a floor and a wall, Int. J. Innovative Technol. Exploring Eng. (IJITEE) 3 (2278–3075) (2013). .7

Y.B.I. Shaheen, E.A. Eltehawy, Structural behaviour of ferrocement channels slabs for low-cost housing, Challenge J. Concr. Res. Lett. 8 (2) (2017) 48–64. .8

P. Desayi, V. Reddy, Strength and behaviour of light-weight ferrocement in tension, in: Proceedings, Second buer- national Symposium on Ferrocement, International Ferrocement Information Centre, Asian Institute of Technology, Bangkok, Thailand, 1985, pp. 61–73. .9

D.G. Gaidhankar, M.S. Kulkarni, A.R. Jaiswal, Ferrocement Composite Beams Under Flexure, IRJET 04 (10) (2017) 117–124. .10

Anuchat Leeanansaksiri, Phaiboon Panyakapo, Anat Ruangrassamee, ‘‘Seismic capacity of masonry infilled RC frame strengthening with expanded metal ferrocement, Eng. Struct. 159 (2018) 110–127. .11

O. Lalaj, Y. Yardim, S. Yilmaz, Recent perspectives for ferrocement, Res. Eng. Struct. Mater. (1) (2015) 11–23, https://doi.org/10.17515/resm2015.04st0123. .12

Constr. Build. Mater. J. 147 (2017) 380–387.

Faris Matalkah, Harsha Bharadwaj, Parviz Soroushian, Wu. Wenda, Areej Almalkawi, Anagi M. Balachandra, Amirpasha Peyvandi, Development of sandwich composites for building .13

I.G. Shaaban, Expanded Wire Fabric Permanent Formwork for Improving Flexural Behaviour of Reinforced Concrete Beams, in: Proceedings of the International Congress: Challenges of Concrete Construction, Dundee, Scotland, UK, September 2002, 2002, pp. 59–70, https://doi.org/10.1680/cmicc.31746.0006. .14

T.A. Abdel, Development of Permanent Formwork for Beams Using Ferrocement Laminates (Ph.D. thesis), Menoufia University, Shebin El-Kom, Egypt, 2006. .15

M. Abdul Kadir, M. Jaafar, Ferrocement in situ permanent formwork, J. Ferrocement 23 (2) (1993) 125–133. .16

G. Mays, R. Barnes, Ferrocement permanent formwork as protection to reinforced concrete, J. Ferrocement 25 (4) (1995) 331–345. .17

M. Abdul Kadir, A. Abdul Samad, Z. Che Muda, A. Ali, Flexural behavior of composite beam with ferrocement permanent formwork, J. Ferrocement 27 (1997) 209–214. .18

E.H. Fahmy, Y.B.I. Shaheen, A.M. Abdelnaby, M.N.A. Zeid, Applying the ferrocement concept in construction of concrete beams incorporating reinforced mortar permanent forms, Int. J. Concr. Struct. Mater. 8 (1) (2014) 83–79. .19

https://doi.org/10.1007/s40069-013-0062-z.

.20 P. Desayi, S.A. El-Kholy, Lightweight fibre-reinforced ferrocement in tension, Cem. Concr. Compos. 13 (1991) 37–48.

.21 M.A. El-Wafa, K. Fukuzawa, Various sizes of wire mesh reinforcement effect on tensile behavior of ferrocement composite plates, in: Proceedings of the 10th International Summer Symposium Organized by Japan Society of Civil Engineers (JSCE), Tokyo, Japan, 2008, pp. 193–196.

.22 M.A. El-Wafa, K. Fukuzawa, Characteristics of ferrocement thin composite elements using various reinforcement meshes in flexure, J. Reinf. Plast. Compos. (2010), https://doi.org/10.1177/0731684410377814.

.23 N.A. Memon, S.R. Sumadi, M. Ramli, Strength and behaviour of lightweight ferrocement, Malaysian J.f Civ. Eng. 18 (2) (2006) 99–108.

.24 Du, W., Yang, C., Wang, C., Pan, Y., Zhang, H., & Yuan, W. (2021). Flexural Behavior of Polyvinyl Alcohol Fiber–Reinforced Ferrocement Cementitious Composite. Journal of Materials in Civil Engineering, 33(4), 04021040.

.25 **ASTM C778 Graded Sand ASTM "**Cement testing standard specifications for standard sand **".**

.26 Egyptian Standards Specification, E.S.S, 4756-11. (2012). Physical and mechanical properties examination of cement, part 1, Cairo.

.27 ASTM C494/C 494 M. (2001). Standard specification for chemical admixtures for concrete. Annual Book of ASTM Standards, 4(2), 9.

.28 Korany, Y.S. (1996) "Repairing Reinforced Concrete Columns Using Ferrocement Laminates", MS thesis submitted to The American University in Cairo, Egypt.

.29 ASTM C618-19. (2019), Standard Specification for Coal Fly Ash and Raw or Calcined Natural Pozzolan for Use in Concrete, ASTM International, West Conshohocken, PA, http://www.astm.org/.

.30 Data sheet of Fine Expanded Perlite from CMB.

.31 Plena Egypt, Delta Sand Bricks Co "The Cost Saving Blocks", a manufacturer's catalogue.

.32 https://www.cmbegypt.com/cmb/datasheets/en/pdf/12-sound-and-thermal-insulation/advefoam.pdf.

.33 E.C.P.203/2007. Egyptian Code of Practice: Design and Construction for Reinforced Concrete Structures. Cairo, Egypt, 2007.

.34 Abaqus User's Guide (2013). Abaqus Documentation User's Guide. s.l.: Dassault Systems, Simulia Corp.